

ChemComm

Accepted Manuscript



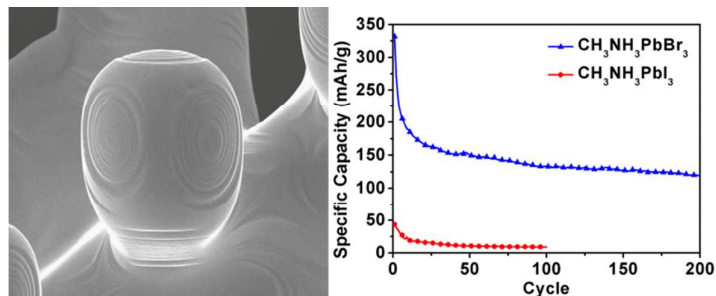
This is an *Accepted Manuscript*, which has been through the Royal Society of Chemistry peer review process and has been accepted for publication.

Accepted Manuscripts are published online shortly after acceptance, before technical editing, formatting and proof reading. Using this free service, authors can make their results available to the community, in citable form, before we publish the edited article. We will replace this *Accepted Manuscript* with the edited and formatted *Advance Article* as soon as it is available.

You can find more information about *Accepted Manuscripts* in the [Information for Authors](#).

Please note that technical editing may introduce minor changes to the text and/or graphics, which may alter content. The journal's standard [Terms & Conditions](#) and the [Ethical guidelines](#) still apply. In no event shall the Royal Society of Chemistry be held responsible for any errors or omissions in this *Accepted Manuscript* or any consequences arising from the use of any information it contains.

A facile rapid hydrothermal method was developed to prepared $\text{CH}_3\text{NH}_3\text{PbBr}_3$ and $\text{CH}_3\text{NH}_3\text{PbI}_3$. The as-prepared products were utilized into lithium batteries as anode materials with good performances obtained. Considering the structural diversity, more hybrid perovskites can be targets for further optimization, indicating their promising potentials in Li-ion battery applications.





Journal Name

COMMUNICATION

Hydrothermal Synthesis of Organometal Halide Perovskites for Li-ion Batteries

Received 00th January 20xx,
Accepted 00th January 20xx

Hua-Rong Xia,^{ab} Wen-Tao Sun^{*ac} and Lian-Mao Peng^{*abc}

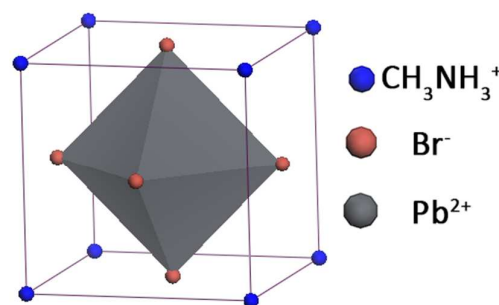
DOI: 10.1039/x0xx00000x

www.rsc.org/

A facile hydrothermal method was developed to prepare $\text{CH}_3\text{NH}_3\text{PbBr}_3$ and $\text{CH}_3\text{NH}_3\text{PbI}_3$. The as-prepared products were utilized into lithium batteries as anode materials with good performances obtained. Considering the structural diversity, more hybrid perovskites can be targets for further optimization, indicating their promising potentials in Li-ion battery applications.

Organic-inorganic hybrid materials, based on a molecular scale composite of inorganic and organic components, have potential applications in many fields such as solar cells¹⁻³, field-effect transistors (FETs)^{4, 5}, light-emitting devices (LEDs)⁶, lasers⁷, photodetectors⁸⁻¹⁰ and so on. These materials combine the properties of inorganic materials (such as high carrier mobility and a wide range of bandgaps) and those of organic materials (such as structural diversity, high efficiency luminescence and plastic mechanical properties^{11, 12}). Some works have attempted to use hybrid organic-inorganic materials (composed of a conducting organic material and an active inorganic material) as lithium storage materials in Li-ion batteries.^{13, 14} However, to date only poor performances were obtained typically such as a specific capacity of less than 50 mAh/g¹³.

Organic-inorganic hybrid perovskites, generally expressed as AMX_3 (A=organic ammonium cation, M=metal cation and X=halide anion), have attracted much attention especially in the field of solar cells with the photoelectric conversion efficiencies of perovskite solar cells increasing from 3.81 % up to 20.1 % within only 5 years^{1-3, 15-17}. The structure of organometal halide perovskite is a three-dimensional framework of corner-connected MX_6 (M=metal cation, X=Cl, Br, I) octahedrons with organic ammonium cations located between the octahedrons. Scheme 1 is a schematic crystal



Scheme 1 Schematic Crystal structure of organometal halide perovskite $\text{CH}_3\text{NH}_3\text{PbBr}_3$.

structure of cubic perovskite $\text{CH}_3\text{NH}_3\text{PbBr}_3$, showing that PbBr_6 octahedrons form the framework with CH_3NH_3^+ locating at the eight vertexes of a cube. As organometal halide perovskite AMX_3 can be regarded as a layered perovskite structure of the alternative arrangement of organic layers and inorganic layers¹¹, similar in topology to Li^+ -insertion compounds such as LiCoO_2 ¹⁸ and graphite¹⁹, it may be possible to use these materials as lithium storage materials in Li-ion batteries. To the best of our knowledge, the lithium storage performance of organometal halide perovskites has not been investigated to date. Moreover, although $\text{CH}_3\text{NH}_3\text{PbBr}_3$ has been prepared by several methods such as spin coating², dip-coating³, thermal evaporation¹⁷, solid-state reaction²⁰ and precipitation reaction²¹, these methods require the use of organic solvents^{2, 3, 17, 20}, or long time for reaction^{2, 3, 20, 21}, or careful adjustment of reaction conditions^{2, 3, 17}. To date, a facile and rapid method is still needed to synthesize organometal halide perovskite materials.

In this paper, $\text{CH}_3\text{NH}_3\text{PbBr}_3$ and $\text{CH}_3\text{NH}_3\text{PbI}_3$ were synthesized by a facile hydrothermal method at low temperature. Furthermore, the as-prepared materials were applied into Li-ion batteries as active materials with lithium storage capabilities investigated. To the best of our knowledge, this is the first time that lithium storage performance of organometal halide perovskites has been reported. The first discharge capacity for $\text{CH}_3\text{NH}_3\text{PbBr}_3$ is up to 331.8 mAh/g. The

^a Key Laboratory for the Physics and Chemistry of Nanodevices, Peking University, Beijing 100871, China.

^b Academy for Advanced Interdisciplinary Studies, Peking University, Beijing 100871, China.

^c Department of Electronics, Peking University, Beijing 100871, China.

* wtaosun@pku.edu.cn; lpeng@pku.edu.cn.

† Electronic Supplementary Information (ESI) available: Experimental details, SEM images and photograph of the perovskite electrode. See DOI: 10.1039/x0xx00000x

capacity of $\text{CH}_3\text{NH}_3\text{PbBr}_3$ fades rapidly in the first 30 cycles, but after that it decreases slowly from 157.4 mAh/g (31st cycle) to 121

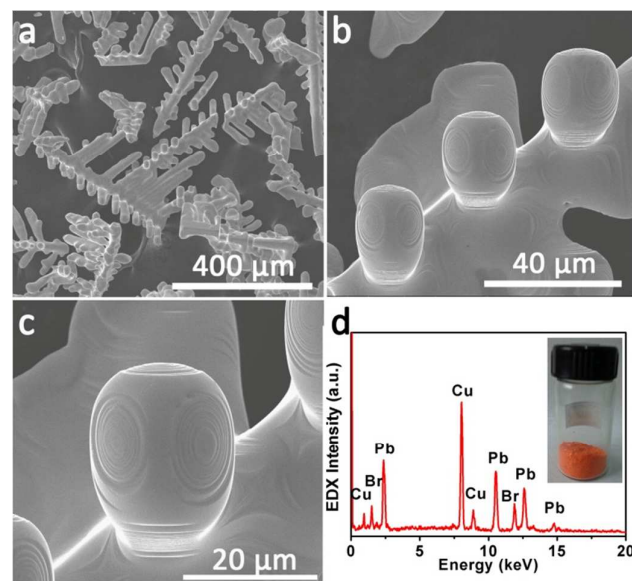


Fig. 1 Morphology and composition characterizations of the hydrothermally synthesized $\text{CH}_3\text{NH}_3\text{PbBr}_3$: (a-c) SEM images with different magnifications; (d) Corresponding EDX spectrum with the photograph of $\text{CH}_3\text{NH}_3\text{PbBr}_3$ inset.

mAh/g (200th cycle) with a relative capacity retention of 76.9 % in the next 170 cycles. Rate performance of the material has also been investigated and the discharge capacities can keep above 210 mAh/g in the first 15 cycles at a smaller current of 20 mA/g or 50 mA/g.

In a typical process, 1-5 g $\text{Pb}(\text{CH}_3\text{COO})_2 \cdot 3\text{H}_2\text{O}$, 15-20 mL HBr solution ($\geq 40\%$) and 3-6 mL CH_3NH_2 alcohol solution (27-32%) were added into a weighing bottle. Then the bottle was put into a 100 mL Teflon-lined stainless steel autoclave and reacted at 150 °C in an oven for 1-12 h. Finally, the products were cooled to room temperature, filtered, washed with superdry isopropanol and dried naturally.

The morphology of the as-prepared $\text{CH}_3\text{NH}_3\text{PbBr}_3$ was characterized by a scanning electron microscopy (SEM). Fig. 1a-c show typical SEM images with different magnifications. As shown in Fig. 1a, the product is composed of some hierarchical rod-like particles with the size of hundreds of micrometers. Closer observation demonstrates that the rod terminals are micrometer-sized head-like spheroids, each with two big eyes and one mouth below them, which seem like statues fabricated by artists' gravers but not a template-free chemical method. The Energy Dispersive X-Ray Spectroscopy (EDX) spectrum is shown in Fig. 1d, which confirms the elemental composition of Pb and Br (Cu from the micro-grid of TEM). This result is reasonable considering the light elements of C and N are difficult to detect. The digital photograph inset in Fig. 1d shows that the obtained product is orange, which is consistent with other reports^{12, 21}.

A Rigaku D/max-rA12kW X-ray diffraction system was used to characterize the crystal structure of the obtained powder.

Further investigation was carried out by X-ray diffraction method to examine the crystal structure of the as-prepared powder and the corresponding result is shown in Fig. 2 with

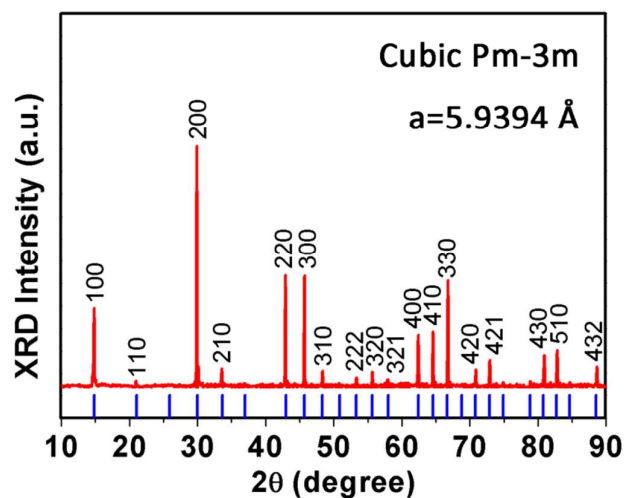


Fig. 2 XRD patterns of the prepared $\text{CH}_3\text{NH}_3\text{PbBr}_3$, which can be indexed as cubic perovskite $\text{CH}_3\text{NH}_3\text{PbBr}_3$ (space group= Pm-3m , $a=5.9394 \text{ \AA}$).

the blue lines corresponding to the simulated XRD patterns. The XRD patterns can be indexed as cubic perovskite structure with $a=5.9394 \text{ \AA}$ (space group= Pm-3m , refined details in Table S1).¹² All XRD peaks can be indexed as cubic perovskite structure, indicating the obtained sample is pure phase cubic perovskite $\text{CH}_3\text{NH}_3\text{PbBr}_3$.

To test if hydrothermal method can be used to synthesize other organometal halide perovskites, $\text{CH}_3\text{NH}_3\text{PbI}_3$ was attempted to prepare by a similar hydrothermal process, except replacing HBr solution with HI solution. (details in Supporting Information).

The obtained product is black, shown as the inset in Fig. 3d. Corresponding SEM images are shown in Fig. 3a-c. The product is composed of some clusters of micrometer-sized wire-like structures. The microwires seem to be with regular shapes, with the diameters of tens of micrometers and the lengths of hundreds of micrometers. XRD characterization was also used to determine the crystal structure of the hydrothermally synthesized sample, with the result shown in Fig. 3d. The XRD patterns can be indexed as tetragonal perovskite $\text{CH}_3\text{NH}_3\text{PbI}_3$ (space group= $4/m\text{cm}$, $a=8.8048 \text{ \AA}$, $b=12.7411 \text{ \AA}$), suggesting perovskite $\text{CH}_3\text{NH}_3\text{PbI}_3$ was also obtained by the hydrothermal method.

Though organometal halide perovskites are considered sensitive to water²²⁻²⁴, high quality perovskite $\text{CH}_3\text{NH}_3\text{PbBr}_3$ with good crystalline was still obtained by the hydrothermal method here. To the best of our knowledge, this is the first time that hydrothermal method was used to synthesize organometal halide perovskites. The successful preparation of $\text{CH}_3\text{NH}_3\text{PbBr}_3$ and $\text{CH}_3\text{NH}_3\text{PbI}_3$ demonstrates that the

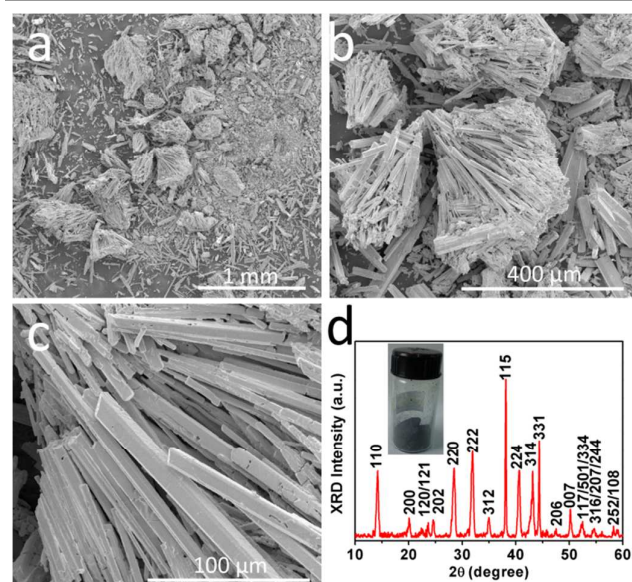


Fig. 3 Characterizations of the $\text{CH}_3\text{NH}_3\text{PbI}_3$ synthesized by a similar hydrothermal process: (a-c) SEM images with different magnifications; (d) XRD patterns with the photograph inset, which can be indexed as tetragonal perovskite $\text{CH}_3\text{NH}_3\text{PbI}_3$ (space group= $I4/mcm$, $a=8.8048$ Å, $b=12.7411$ Å).

hydrothermal method developed here is facile but effective to synthesize organometal halide perovskites.

To investigate the lithium storage performance of the as-synthesized samples, standard RS2032 coin cells were assembled in an argon-filled glove box with the moisture content less than 1 ppm. The test electrodes were composed of $\text{CH}_3\text{NH}_3\text{PbBr}_3$ (or $\text{CH}_3\text{NH}_3\text{PbI}_3$), conductive carbon black and PVDF binder with an 80:10:10 mass ratio. The corresponding SEM images and photographs of perovskite $\text{CH}_3\text{NH}_3\text{PbBr}_3$ electrodes are shown in Fig. S1-2 (Supporting Information). Lithium metal was used as the counter electrode and 1 mol/L LiPF_6 solution in ethylene carbonate + ethylmethyl carbonate + dimethyl carbonate (EC+EMC+DMC, volume ratio=1:1:1) was selected as the electrolyte. Constant current charge-discharge performance of the coin cells were carried out with a LAND BT2013A 8-channel battery test system (Wuhan Rambo Testing Equipment Co., Ltd.) in the voltage range of 0.1-1.5 V. Cyclic voltammetry was measured on a CHI660C electrochemical workstation at a sweep voltage range of 0.01-2.0 V with the rate of 1 mV/s.

First charge-discharge profiles of the prepared perovskite $\text{CH}_3\text{NH}_3\text{PbI}_3$ and $\text{CH}_3\text{NH}_3\text{PbBr}_3$ at a constant current density of 200 mA/g are shown in Fig. 4a. The first discharge capacity of $\text{CH}_3\text{NH}_3\text{PbI}_3$ is 43.6 mAh/g, which is comparable to that of other organic-inorganic hybrids with capacities less than 50 mAh/g.^{13,14} While the first discharge capacity of $\text{CH}_3\text{NH}_3\text{PbBr}_3$ can be up to 331.8 mAh/g, which is much larger than that of $\text{CH}_3\text{NH}_3\text{PbI}_3$. Although the detailed reasons for the improved performance of $\text{CH}_3\text{NH}_3\text{PbBr}_3$ are unknown, the lower molecular weight of $\text{CH}_3\text{NH}_3\text{PbBr}_3$ and larger first charge-discharge efficiency shown in Fig. 4a, must make a significant

contribution to the improved capacity. The charge-discharge voltage plateaus in the charge-discharge profiles indicate that

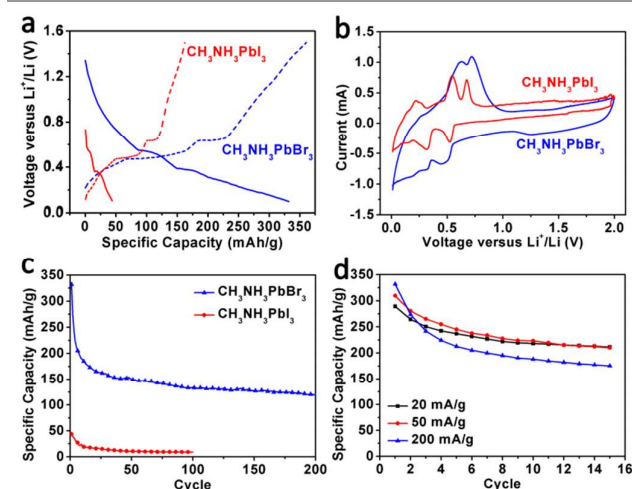


Fig. 4 Electrochemical characterizations of the Li-ion batteries made of perovskite $\text{CH}_3\text{NH}_3\text{PbBr}_3$ and $\text{CH}_3\text{NH}_3\text{PbI}_3$: (a) Charge-discharge profiles; (b) Cyclic voltammetry curves; (c) Cycle performances; (d) Rate performance of perovskite $\text{CH}_3\text{NH}_3\text{PbBr}_3$.

the oxidation or reduction reactions may happen at the corresponding voltages, which can be well corresponding to the oxidation or reduction reaction peaks in the cyclic voltammetry curves shown in Fig. 4b.

The cycle performances of the two compounds are also compared in Fig. 4c. Both of the capacities decay much in the first 30 cycles, but decrease slowly after that. Only a capacity of 9 mAh/g is left after 100 cycles for perovskite $\text{CH}_3\text{NH}_3\text{PbI}_3$. While the 100th discharge capacity for the corresponding perovskite $\text{CH}_3\text{NH}_3\text{PbBr}_3$ is 133.7 mAh/g, and the 200th discharge capacity is still as large as 121 mAh/g. For $\text{CH}_3\text{NH}_3\text{PbBr}_3$, the discharge capacity decreases slowly from 157.4 mAh/g (31th cycle) to 121 mAh/g (200th cycle) with a relative capacity retention of 76.9 % in this 170 cycles. Compared with $\text{CH}_3\text{NH}_3\text{PbI}_3$, we just replaced I^- with Br^- in the perovskite $\text{CH}_3\text{NH}_3\text{PbX}_3$ (X=halide anion), but the performance of perovskite $\text{CH}_3\text{NH}_3\text{PbBr}_3$ was significantly enhanced. Considering the structural diversity of organometal halide perovskite AMX_3 (A=organic ammonium cation, M=metal cation and X=halide anion), achieving much better performance is possible for Li-ion battery applications.

To characterize the rate performance, cycle performances at different charge-discharge current densities were also tested and the corresponding results are shown as Fig. 4d. When the test current is 20 mA/g or 50 mA/g, the discharge capacities are above 210 mAh/g in the first 15 cycles. When charged/discharged at a much larger current density of 200 mA/g, the 15th discharge capacity can still retain 175.5 mAh/g, which is equivalent to the theoretical capacity of commercial $\text{Li}_4\text{Ti}_5\text{O}_{12}$ (175 mAh/g).^{25, 26} The good rate performance indicates that $\text{CH}_3\text{NH}_3\text{PbBr}_3$ can be charged/discharged at different rates without much capacity decay, showing structural stability for Li-ion battery applications.

Conclusions

In conclusion, $\text{CH}_3\text{NH}_3\text{PbI}_3$ and $\text{CH}_3\text{NH}_3\text{PbBr}_3$ were synthesized by a facile hydrothermal method and utilized as active materials in Li-ion battery with reversible charge-discharge capacities. The first discharge capacity for $\text{CH}_3\text{NH}_3\text{PbBr}_3$ (331.8 mAh/g) is much larger than that for $\text{CH}_3\text{NH}_3\text{PbI}_3$ (43.6 mAh/g) at a current density of 200 mA/g. Both capacities decay rapidly in the first 30 cycles but decrease slowly after that. The 15th discharge capacity of $\text{CH}_3\text{NH}_3\text{PbBr}_3$ is 175.5 mAh/g, which is equivalent to the theoretical capacity of commercial $\text{Li}_4\text{Ti}_5\text{O}_{12}$. After 200 charge-discharge cycles, the capacity is still 121 mAh/g, with a 76.9 % relative capacity retention to the 31st discharge capacity (157.4 mAh/g). Compared to $\text{CH}_3\text{NH}_3\text{PbI}_3$, the significantly enhanced performance of $\text{CH}_3\text{NH}_3\text{PbBr}_3$ indicates that the composition of organometal halide perovskite AMX_3 plays an important role in the lithium storage performance. Considering the structural diversity, better performance may be achieved by tuning the composition, which suggesting that organic-inorganic perovskite materials have promising potentials in lithium storage applications.

Acknowledgements

This work was supported by the Ministry of Science and Technology (Grant No. 2011CB933002 and 2012CB932702) and the National Science Foundation of China (Grant No. 61306079, 61171023).

Notes and references

1. A. Kojima, K. Teshima, Y. Shirai and T. Miyasaka, *J. Am. Chem. Soc.*, 2009, **131**, 6050-6051.
2. M. M. Lee, J. Teuscher, T. Miyasaka, T. N. Murakami and H. J. Snaith, *Science*, 2012, **338**, 643-647.
3. J. Burschka, N. Pellet, S.-J. Moon, R. Humphry-Baker, P. Gao, M. K. Nazeeruddin and M. Gratzel, *Nature*, 2013, **499**, 316-319.
4. C. R. Kagan, D. B. Mitzi and C. D. Dimitrakopoulos, *Science*, 1999, **286**, 945-947.
5. D. B. Mitzi, C. D. Dimitrakopoulos, J. Rosner, D. R. Medeiros, Z. Xu and C. Noyan, *Adv. Mater.*, 2002, **14**, 1772-1776.
6. Z.-K. Tan, R. S. Moghaddam, M. L. Lai, P. Docampo, R. Higler, F. Deschler, M. Price, A. Sadhanala, L. M. Pazos, D. Credgington, F. Hanusch, T. Bein, H. J. Snaith and R. H. Friend, *Nat. Nano.*, 2014, **9**, 687-692.
7. Q. Zhang, S. T. Ha, X. F. Liu, T. C. Sum and Q. H. Xiong, *Nano Lett.*, 2014, **14**, 5995-6001.
8. H.-R. Xia, J. Li, W.-T. Sun and L.-M. Peng, *Chem. Commun.*, 2014, **50**, 13695-13697.
9. X. Hu, X. Zhang, L. Liang, J. Bao, S. Li, W. Yang and Y. Xie, *Advanced. Funct. Mater.*, 2014, **24**, 7373-7380.
10. L. Dou, Y. Yang, J. You, Z. Hong, W.-H. Chang and G. Li, *Nat. Commun.*, 2014, **5**, 1-6.
11. D. B. Mitzi, in *Progress in Inorganic Chemistry, Vol 48*, ed. K. D. Karlin, 1999, vol. 48, pp. 1-121.
12. L. C. Schmidt, A. Pertegás, S. González-Carrero, O. Malinkiewicz, S. Agouram, G. Mínguez Espallargas, H. J. Bolink, R. E. Galian and J. Pérez-Prieto, *J. Am. Chem. Soc.*, 2014, **136**, 850-853.
13. A. Jaffe and H. I. Karunadasa, *Inorganic Chemistry*, 2014, **53**, 6494-6496.
14. M. Lira-Cantú and P. Gómez-Romero, *Chem. Mater.*, 1998, **10**, 698-704.
15. M. A. Green, K. Emery, Y. Hishikawa, W. Warta and E. D. Dunlop, *Prog. Photovoltaics: Research and Applications*, 2015, **23**, 1-9.
16. H. Zhou, Q. Chen, G. Li, S. Luo, T.-b. Song, H.-S. Duan, Z. Hong, J. You, Y. Liu and Y. Yang, *Science*, 2014, **345**, 542-546.
17. M. Liu, M. B. Johnston and H. J. Snaith, *Nature*, 2013, **501**, 395-398.
18. T. Wei, R. Zeng, Y. Sun, Y. Huang and K. Huang, *Chem. Commun.*, 2014, **50**, 1962-1964.
19. F. Wang, J. Graetz, M. S. Moreno, C. Ma, L. Wu, V. Volkov and Y. Zhu, *Acs Nano*, 2011, **5**, 1190-1197.
20. L. Chen, F. Tang, Y. Wang, S. Gao, W. Cao, J. Cai and L. Chen, *Nano Res.*, 2015, **8**, 263-270.
21. A. Poglitsch and D. Weber, *J. Chem. Phys.*, 1987, **87**, 6373-6378.
22. X. Dong, X. Fang, M. Lv, B. Lin, S. Zhang, J. Ding and N. Yuan, *J. Mater. Chem. A*, 2015, **3**, 5360-5367.
23. Y. S. Kwon, J. Lim, H.-J. Yun, Y.-H. Kim and T. Park, *Energy Environ. Sci.*, 2014, **7**, 1454-1460.
24. S. N. Habisreutinger, T. Leijtens, G. E. Eperon, S. D. Stranks, R. J. Nicholas and H. J. Snaith, *Nano Lett.*, 2014, **14**, 5561-5568.
25. Y. Ma, B. Ding, G. Ji and J. Y. Lee, *Acs Nano*, 2013, **7**, 10870-10878.
26. S. Chen, Y. Xin, Y. Zhou, Y. Ma, H. Zhou and L. Qi, *Energy Environ. Sci.*, 2014, **7**, 1924-1930.